

INFLUENCE OF VANE CARRIER DESIGN IN STEAM EXTRACTION MODULES ON THE FLOW CONDITIONS OF THE SUBSEQUENT TURBINE STAGE

A. Schramm – D. Engelmann – T. Polklas – O. Brunn* – R. Mailach*

Ruhr-Universität Bochum, Chair of Thermal Turbomachinery, 44801, Bochum, Germany,
andreas.schramm@rub.de

* MAN Diesel & Turbo SE, 46145, Oberhausen, Germany

ABSTRACT

Extraction modules allow the regulated extraction of large steam quantities on certain enthalpy levels. While extraction steam is lead out of the turbine with an outlet flange, the remaining steam flows through control valves and adjacent diffusers into an annular inlet chamber. Depending on the valve lift, the compact and asymmetric design of the extraction module causes a strongly disturbed incoming flow of the following guide vanes.

The current work focusses on improving the inflow of the subsequent guide vanes with regard to uniformity of mass flux and flow inlet angle.

As the simulation results illustrate, modification of horizontal as well as vertical valve position can lead to significant variations in distribution of mass flux and flow inlet angle. Furthermore, intense contouring of the vane carrier can minimize the influence of the turbulent steam jet, if compact design is required.

NOMENCLATURE

A	-	area
B	-	neck span
c	m/s	velocity
D		ratio of valve seat distance
e	m	eccentricity
F	N	vane force
G	kg/m ² s	mass flux
H _{Blade}	m	blade height
L	m	distance valve seat to hub
K		ratio of neck span
Ma	-	Mach number
\dot{m}	kg/s	mass flow
N	rpm	rotational speed
p	Pa	pressure
R	m	radius
Re	-	Reynolds number
S _{0,Tang}	-	geometric swirl number
t	m	pitch
y ⁺	-	dimensionless wall distance
X	-	axis of rotation

Greek Symbols

α	deg	flow inlet angle
φ	deg	circumferential angle
ρ	kg/m ³	density

Subscripts

ax	axial
BASE	base model
DifOut	outlet diffuser
m	meridional
out	outlet
rad	radial
tang	tangential
VAR	variant

Abbreviations

IF	interface
IP	intermediate pressure
HP	high pressure
HVP	horizontal valve position
VCS	vane carrier shape
VVP	vertical valve position

INTRODUCTION

Modular design concepts are used to meet the various requirements concerning industrial steam turbines. Steam admission and extraction modules ensure the optimum integration of industrial steam turbines into power plants or chemical engineering processes. In extraction modules valves regulate the amount of steam extracted from the turbine expansion path. As a result of the intense flow acceleration within the control valves a turbulent jet arises in the diffusers, directly influencing the flow in front of the guide vanes. Hence, in addition to efficiency loss, partially strong structure-mechanical blade row loads can occur.

Many investigations on inlet chambers as well as on control valves exist as of today. Nevertheless, no published studies about the design of extraction modules in industrial turbines are available at present. Kovats (1979), Lüdtkke (1985), Traupel (2001), van den Braembussche (2006) and Sievert (2006) suggest several design guidelines for inlet chambers. Kovats (1979) detects a significant decrease of flow losses as a result of constricting the casing in flow direction. Lüdtkke (1985) analyses an inlet chamber with one radial flange and separation sheet to suppress asymmetric flow conditions. He detects a three-dimensional flow structure with two contra-rotating vortices at 30 deg and 330 deg circumferential angle. Traupel (2001) and van den Braembussche (2006) recommend to increase the ratio of inlet- to outlet area to realize an accelerated flow. Greim et al. (1999), Kocarnik and Jirku (2005) and Sievert (2006) give different suggestions for the casing design to improve the deflection of steam from radial into axial direction. Hecker (2011) compares two different types of inlet chambers for intermediate pressure turbines regarding to aerodynamic and mechanical points of view: ring type inlet and inlet scroll. Due to the strong structure mechanical elongation of an inlet scroll and the resulting increase of tip clearance, he recommends the application of an elliptical inlet with neckings at 0 deg and 180 deg circumferential angle.

Tajc et al. (2003), Zhang et al. (2004) and Morita et al. (2004) study the flow characteristics around control valves at different valve openings experimentally and numerically. Tajc et al. (2003) describe the redesign process for a control valve of a turbine, operating with saturated steam at small openings, to decrease the intensive vibrations in the inlet piping system. As the experimental study of Zhang et al. (2004) shows, specific valve lifts could induce pressure oscillations with asymmetric flow character resulting in plug vibrations. Morita et al. (2004) detect in experiments at middle valve opening a spike-type pressure fluctuation that rotates circumferentially, sometimes changing its rotation direction suddenly or remaining at the same circumferential position. In a numerical study he states the single-sided detachment from the valve seat and the associated interaction of the steam jets as one possible reason for the spike-type fluctuations.

In this contribution a commercial 3D RANS CFD-solver (ANSYS CFX 13) is used to analyse the influence of valve positions and vane carrier shapes on the flow within the annular inner casing, and in front of the subsequent guide vanes. The main goals of this study are an improvement of uniformity of mass flux and incidence angle in circumferential direction, as well as a reduction of unsteady structure-mechanical blade row loads. In the first part the geometry of the investigated domain is described along with the steady and unsteady flow conditions of the base design. The second part deals with variation of the control valve position and shape modification of the vane carrier design.

NUMERICAL INVESTIGATIONS ON THE BASE EXTRACTION MODULE

Figure 1 shows an industrial steam turbine with two steam extraction modules. Due to the possible non-uniformity at high steam parameters behind the high pressure (HP) module, the first extraction module includes a control stage. A second extraction module after the intermediate pressure (IP) module is used to extract steam at lower parameters. Figure 2 depicts the model of the investigated extraction module. It allows a steam extraction at medium steam parameters (~ 30 bar; 600 K), and is arranged between the HP and the IP module of an industrial steam turbine. Two Control valves regulate the quantity of steam vertically extracted through the outlet flange. The remaining steam flows through a short diffuser into an inlet chamber to ensure a uniform

distribution of steam in circumferential direction in front of the subsequent guide vane row. On one hand the labyrinth sealing is used to separate the two domains with different pressure levels. On the other hand the sealing ensures a minimum steam quantity to supply the subsequent LP turbine stages in case of closed control valves.

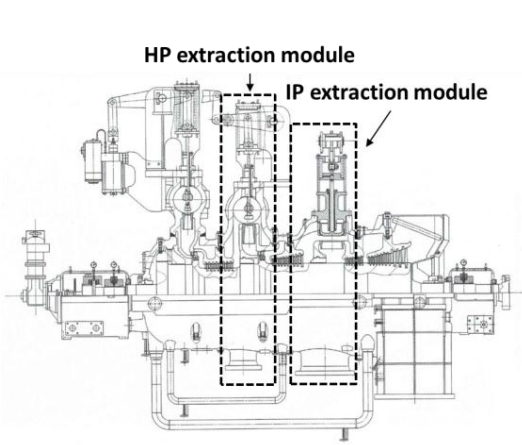


Figure 1: Industrial steam turbine

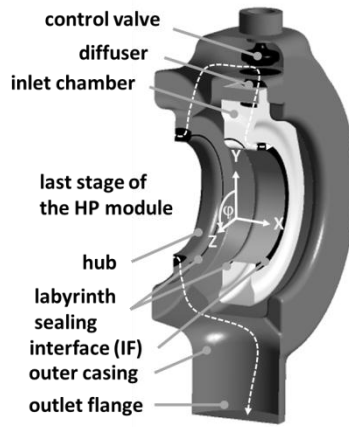


Figure 2: Investigated IP extraction module

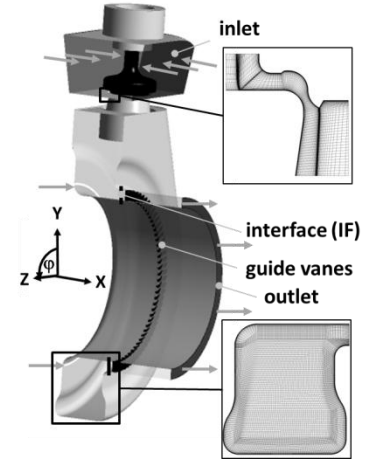


Figure 3: Investigated flow domain

The investigated flow domain, the flow direction and drawings of the grid are shown in Figure 3. The complete domain is modelled and solved numerically by using a structured mesh with roughly 20 million grid points. Flow domains of the valves, diffusers and inlet chamber are created with ICEM CFD and consist of approximately 15 million nodes. They are connected with an interface (IF) to the mesh of first guide vane row with 84 blades, generated with TURBOGRID and possessing about 50,000 nodes for each passage. An axial distance of six times the chord length between the evaluation and the outlet plane is realized to suppress potential impact from the outlet boundary condition, as Kalkkuhl et al. (2012) suggest. A fine grid structure in the region of the control valves and the adjacent diffusers ensures a good prediction of the complex flow pattern. The maximum y^+ value is about three in the gap between valve and valve seat and not greater than 50 in the subsequent inlet chamber. The final level of overall mass flow convergence was $1E-04$ with an imbalance less than 0.5%. Table 1 assembles the most important design parameters of the industrial steam turbine. In table 2 the used boundary conditions are listed.

Table 1: List of design parameters

Design speed	6548 rpm
Design mass flow	80 kg/s
Power	38.5 MW
Degree of reaction	0.5
Flow coefficient $\varphi/\varphi_{ref, 1st\ HP\ stage}$	0.62
Enthalpy coefficient $\Psi/\Psi_{ref, 1st\ HP\ stage}$	1.4

Table 2: List of boundary conditions

Fluid	Steam IAPWS-IF97
Heat transfer model	Total energy
Turbulence model	Shear stress transport (SST)
Pressure ratio $[p_{in}/p_{out}]$	1.8
Inlet boundary	Total pressure & temperature, normal to boundary
Inlet boundary labyrinth sealing	Mass flow rate
Outlet boundary	Static pressure condition
Wall boundary	Adiabatic, smooth, non-slip condition
Valve lift (rating)	18 %

Steady-state results of the base model

Different flow patterns occur within the diffusers depending on the valve lift (see Zhang et al. 2004). In rated operation at a valve lift of 18%, the flow detaches from the valve seat whereupon the flow pattern becomes strongly unsteady, generating the maximum residues during the steady state simulations. Transient simulations show a partially rotating separation inside the diffuser, with sometimes changing rotational direction or remaining circumferential position, as Morita (2004) describes. According to the flow pattern in circumferential direction a detached jet [A] or an attached jet [B] arises (see Figure 4 right side). Due to the compact design of the base model, the jet is even retained in the inlet chamber, subsequently influencing the flow in front of the guide vanes. The reasons for the different flow pattern behind the diffusers are the rotation of the hub, the rotating separation at the valve seat and the transient vortex structure beside and between the steam jets (see Figure 4 left side).

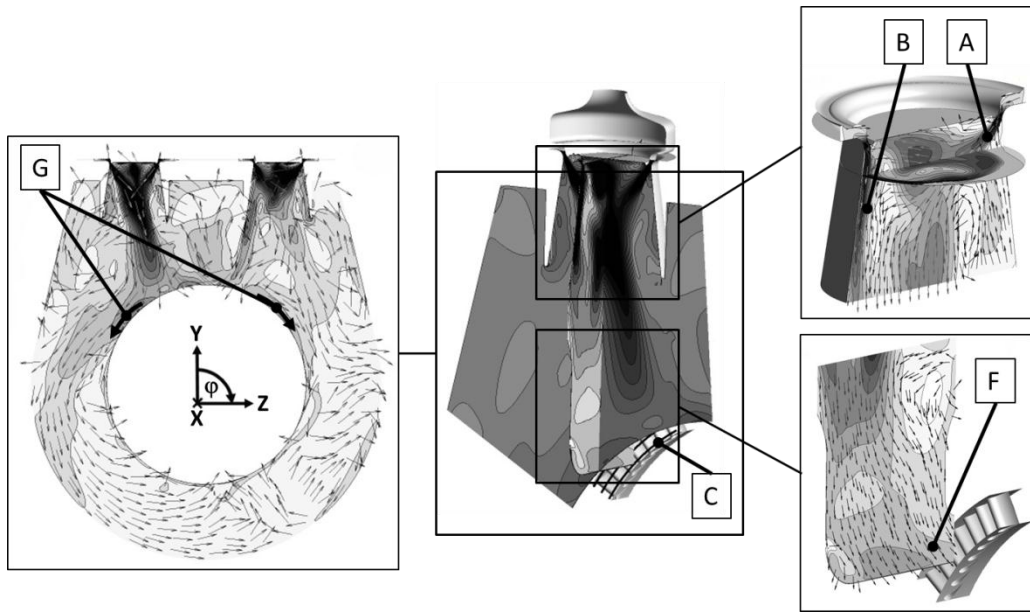


Figure 4: **Mach number distribution and vector plot on midplane and diffuser midplane**

In order to evaluate the flow uniformity in circumferential direction upstream of the guide vanes, the mass flux related to the outlet mass flux is calculated (see equation 1). Due to the constant valve lift of 18% and the unmodified outlet cross-section (see Figure 3), mass flow and outlet area are constant in all variations.

$$\frac{G}{G_{\text{Out}}} = \frac{\rho \cdot c_m \cdot A_{\text{Out}}}{\dot{m}} \quad (1)$$

A possible flow incidence in front of the guide vanes leads to an increasing flow loss, and hence to a decreasing guide vane efficiency. Thus, the distribution of flow inlet angle in circumferential direction in equation 2 is a second assessment criterion for flow uniformity.

$$\alpha = 90^\circ + \arctan\left(\frac{c_{\text{tang}}}{c_m}\right) \quad (2)$$

Figures 5 and 6 illustrate the results of the steady-state simulation of the base model. Figure 5 depicts the dimensionless mass flux at 10%, 50% and 90% blade height in front of the first guide vane row in circumferential direction (see Figure 4 [C]). The potential effect of the guide vanes

leads to a reduction of mass flux in spatial direction, depending on the number of vanes (see Figure 5[D]). Furthermore Figure 5 [E] indicates massive disturbances at 30 deg and 330 deg circumferential angle, conditioned by the position of the control valves. Due to the radial inflow from the diffusers, the steam is pressed directly to the hub respectively in the guide vane cross section (see Figure 4 [F]). Additionally, the considerable radial velocity component leads to a separation from the casing, explaining the increased mass flux at the hub (Figure 4 right, 5 [F]).

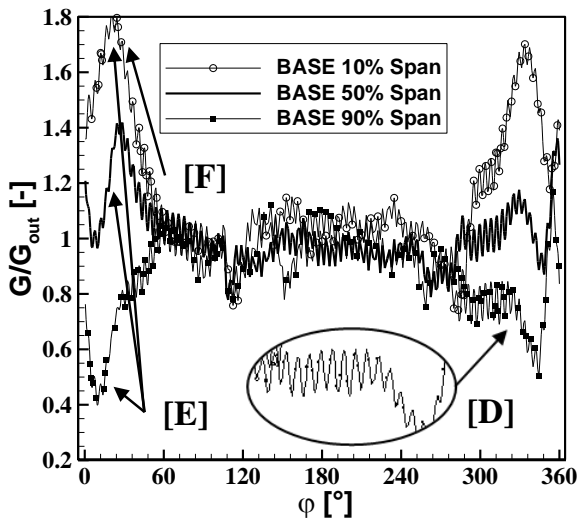


Figure 5: Dimensionless mass flux at 10%, 50% and 90% guide vane height

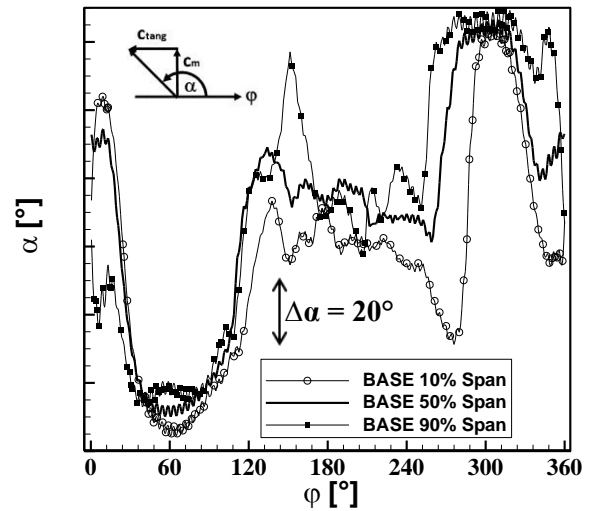


Figure 6: Flow inlet angle at 10%, 50% and 90% guide vane height

Figure 6 illustrates the flow inlet angle in front of the first guide vane row, related to the circumferential angle at 10%, 50% and 90% blade height. Significant incidence becomes obvious at circumferential positions of 60 deg and 300 deg. Steam remaining in the inlet chamber is deflected in circumferential direction (see Figure 4 left [G]) and subsequently the high tangential velocity component generates the high incidence.

The spatial non-uniformity in mass flux and flow inlet angle can result in strong structure-mechanical blade loads in circumferential direction. According to the momentum equation the blade force correlates directly with the valve lift, respectively the mass flow rate advecting the inlet chamber. Figures 7 and 8 depict the resulting blade force and the components in axial, tangential and radial direction at a valve lift of 18%.

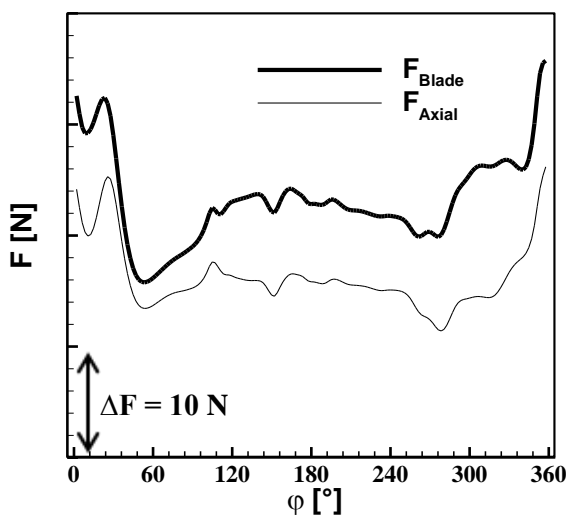


Figure 7: Resulting and axial blade force

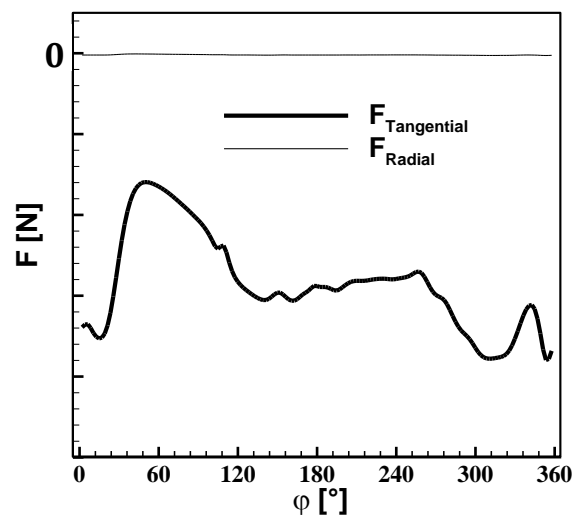


Figure 8: Tangential and radial blade force

The distribution of resulting-, axial- and tangential blade force is given by equations 3, 4 and 5. Axial force is mainly characterized by the pressure distribution in front of the guide vanes. Figure 7 shows nearly the same trends for resulting and axial force. Due to slightly higher pressure the axial force increases between the steam jets.

$$F_{ax} = \dot{m} \cdot \Delta c_{ax} + \Delta p \cdot t \cdot H_{Blade} \quad (3)$$

Equation 4 implies that the tangential blade force is dependent on the change of the tangential velocity component while crossing the guide vane. Based on the fixed blade exit angle, the tangential blade force is almost only dependent of the flow inlet angle.

$$F_{tang} = \dot{m} \cdot \Delta c_{tang} \quad (4)$$

Figure 8 confirms this assumption. The considerable flow incidence, at circumferential positions of 60 deg and 300 deg (see Figure 6), leads to a spatial non-uniformity of the tangential force. A decreasing flow inlet angle induces a suction side inflow and a decreasing tangential force, whereas an increasing flow inlet angle causes pressure side inflow and an increasing tangential force contrary to the circumferential direction. Due to the negligible radial component, the resulting force is given by equation 5.

$$F_{Blade} = \sqrt{F_{ax}^2 + F_{tang}^2} \quad (5)$$

Thus the difference between resulting and axial force corresponds to the tangential force.

Comparison of steady state and transient results of the base model

The influence of the unsteady flow in the diffuser on the incoming flow in front of the guide vanes is investigated in Figures 9 and 10 by comparing the steady-state with transient simulation results, with regard to the distribution of mass flux and flow inlet angle.

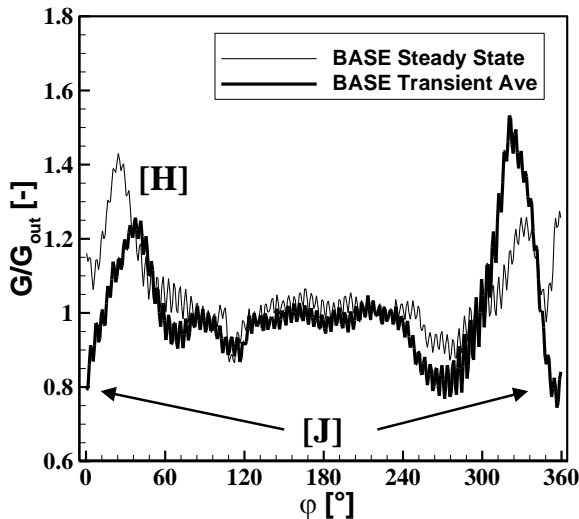


Figure 9: Radially averaged, dimensionless mass flux

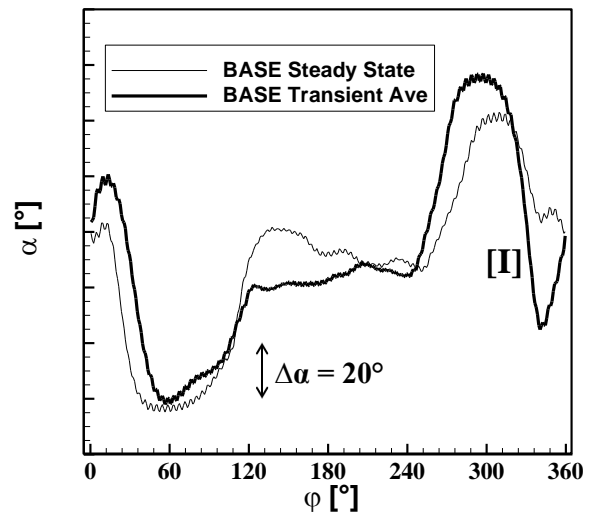


Figure 10: Radially averaged inlet angle

The results shown in Figures 9 and 10 are area averaged on one degree segments in radial direction. Furthermore transient results are time averaged over a period of one turn of the hub. They

confirm the already obtained influence of the valve position and show the same trends like the steady state results. However, the disturbance at minor circumferential angle shifts about 15 deg (see Figure 9 [H]). The flow inlet angle given in Figure 10 shows a good concordance between the steady-state and the transient results. An exception is the region between the steam jets, where transient behaviour of steam jets and resulting vortex structure in between lead to a shift of flow inlet angle (see Figure 10 [I]). As a consequence of the comparison it is obvious that the results of the steady-state simulation are sufficient to predict the disturbances in mass flux and flow inlet angle distributions appearing in circumferential direction.

VARIATION OF THE EXTRACTION MODULE DESIGN

In order to attenuate the strong spatial non-uniformity upstream of the guide vane row ensuing from the base model, the influence of different geometry variants is analysed. Beside the vertical (VVP) and the horizontal valve position (HVP), the influence of intense contouring at the transition to the vane carrier (VCS) is studied (see Figure 11). For this purpose, the investigated domain is divided into three regions: control valve, neck and inlet chamber. This ensures a wide range of possible variations (see Figure 12).

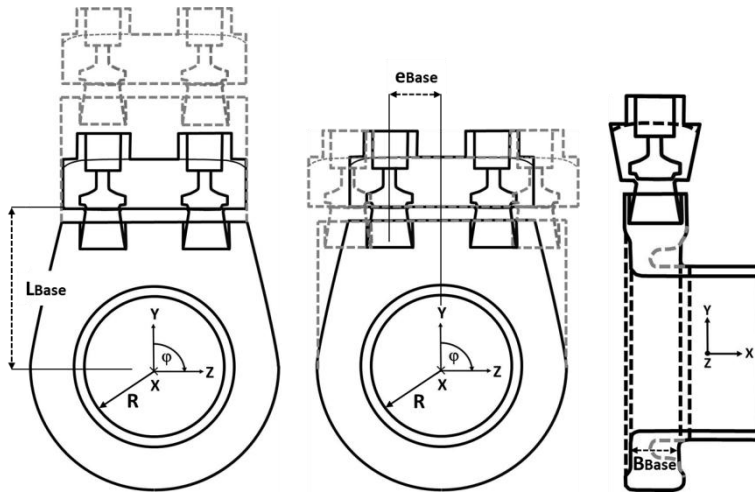


Figure 11: Investigated design variations (VVP, HVP, VCS)

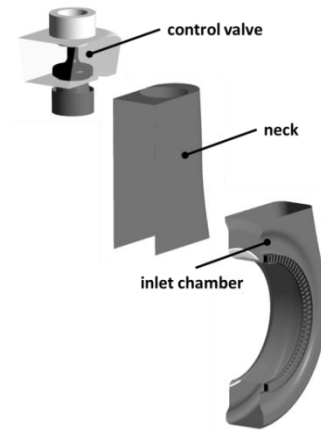


Figure 12: Block structure

After the variation of one single mesh part, subsequently the various mesh parts are reconnected, avoiding interpolation faults. The geometry variants are simulated steady-state with the boundary conditions given in Table 2. As a consequence of vertical and horizontal valve position variation, asymmetric flow pattern is possible. For that reason a 360 deg model is simulated. Within the study of intense casing contouring a 180 deg model with geometric vertical symmetry is used, thus asymmetric flow pattern still exists, but has no decisive impact on the result of this study. The result is verified on a 360 deg model. Studies on the base model show the largest non-uniformity in the distribution of mass flux and flow inlet angle near the hub. Hence, effects of modification are discussed and assessed at constant radius of 10 % guide vane height for the two most representative variants in the following sections.

Influence of vertical valve position (VVP)

In this study, starting from the base model, the distance between hub and valve seat is gradually enlarged, given by the ratio in equation 6. The shape of valve and inlet chamber as well as the horizontal valve position remains unaffected. So only the region of neck has to be adapted. Table 3 on the right side provides an overview of the simulated variants.

Table 3: design variants VVP

D_{Base}	1
D_{VVP2}	1.4
D_{VVP4}	1.8

$$D = \frac{L_{VAR}}{L_{Base}} \quad (6)$$

Figure 13 illustrates a significant improvement of mass flux distribution. Due to the enlarged distance between hub and valve seat the momentum of the steam jet is distributed more evenly over a wider cross section through turbulent diffusion, under the assumption of conservation of momentum (e.g. Schlichting, 1979). Hence the area increase of the neck leads to a reduction of the high radial velocity component downstream the diffusers and finally to a homogenised radial velocity distribution at the end of the neck. That way non-uniformity in mass flux distribution resulting from valve position could be avoided.

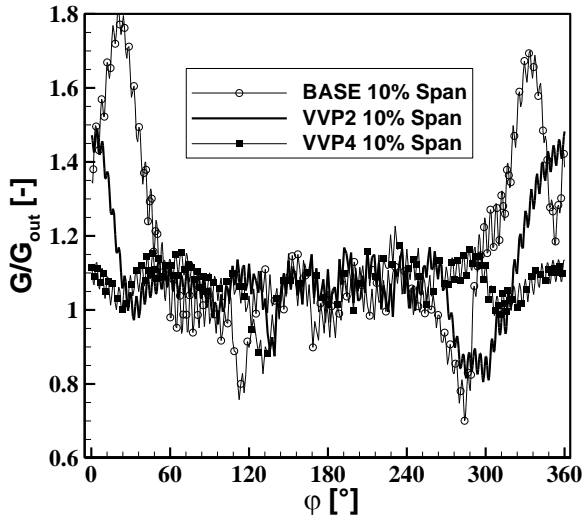


Figure 13: Comparison of dimensionless mass flux at 10% guide vane height

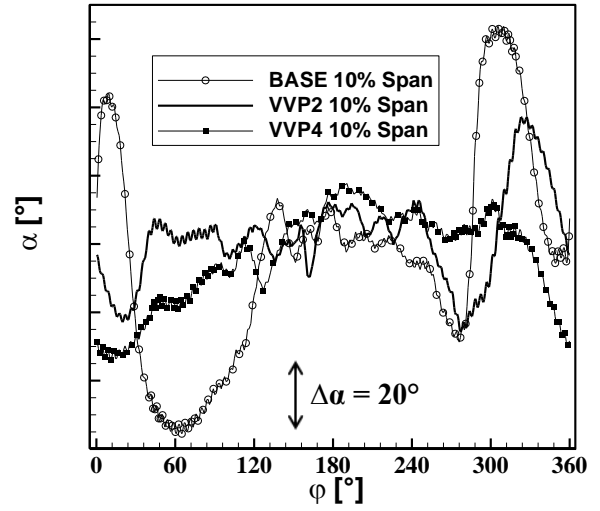


Figure 14: Comparison of flow inlet angle at 10% guide vane height

A more evened distribution of the radial velocity at the end of the neck leads to a more balanced ratio between meridional and tangential velocity component in front of the guide vanes, and consequently to an improved flow inlet angle (shown in Figure 14).

Influence of horizontal valve position (HVP)

To investigate the influence of the horizontal valve position, the arrangement is changed two times with the result that VHP 3 is almost tangential to the hub. Assuming a balanced velocity distribution at the diffuser outlet, the geometric swirl number is defined by equation 7. The dimensionless swirl numbers for all variants, defining the tangential positions of the valves to the hub are given in Table 4.

$$S_{0,Tang} = \frac{e_{VAR} \cdot \pi \cdot R}{\sum A_{DifOut}} \quad (7)$$

Table 4: design variants VHP

$S_{0,Tang, Base}$	6
$S_{0,Tang, VHP2}$	9.4
$S_{0,Tang, VHP3}$	11.1

As a consequence of the tangential valve position, the flow direction is changed from hub to the lateral parts of the inlet chamber. Thus, it is possible to direct as much steam as possible in circumferential direction, causing a regular inflow, too. However, simultaneously a sink of mass flux between the two valves (see Figure 15[K]) is generated, whereby use of a smaller, centrally positioned additional valve should be examined. As Figure 16 depicts, a more tangential

arrangement induces mutually interference of the two valves below the hub, effecting a flow transition, respectively an asymmetric flow pattern. In order to suppress a possible flow transition necking of casing in flow direction (Lüdtke, 1985) should be tested, too.

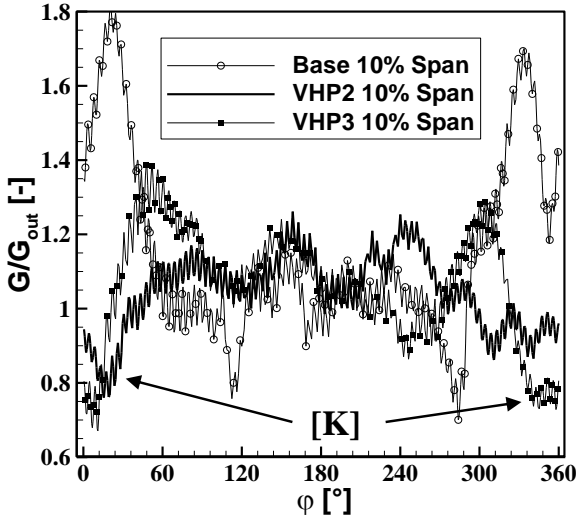


Figure 15: Comparison of dimensionless mass flux at 10% guide vane height

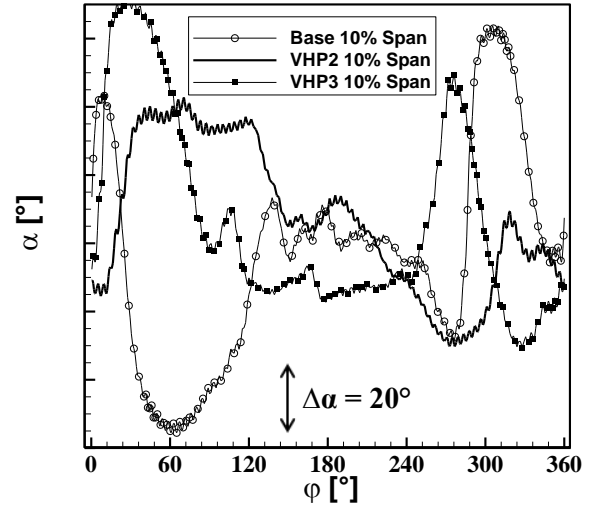


Figure 16: Comparison of flow inlet angle at 10% guide vane height

Influence of intense contouring of the vane carrier (VCS)

In the next chapter the influence of neck constriction in axial direction within the inlet chamber in front of the deflection from radial to axial direction, as shown in Figure 11 on the right side is studied. In this regard horizontal and vertical valve position remains unaffected. The dimension of the variants related to the base geometry can be extracted from Table 5. The impact of the variants is analysed on a 180 deg model.

Table 5: design variants VCS

K_{Base}	1
K_{VCS2}	0.77
K_{VCS4}	0.4

$$K = \frac{B_{VAR}}{B_{Base}} \quad (8)$$

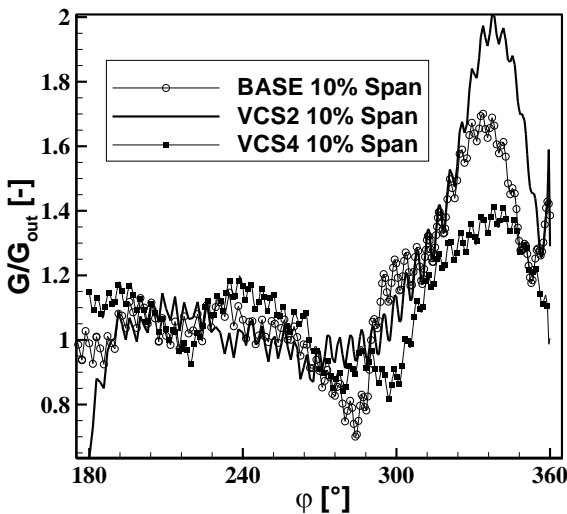


Figure 17: Comparison of dimensionless mass flux at 10% guide vane height

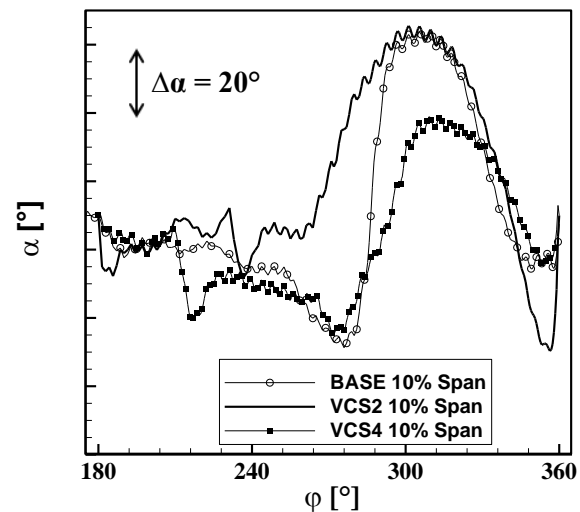


Figure 18: Comparison of flow inlet angle at 10% guide vane height

As Figure 17 indicates, the constriction of variant VCS2 causes an increasing radial velocity component and consequently a rise of mass flux near the valve. Further constricting of the inlet chamber enforces deflection of steam in circumferential direction, minimizing the non-uniformity in mass flux distribution. Figure 18 illustrates that there is nearly no significant improvement of the flow inlet angle distribution. The compactness still leads to a high tangential velocity component in the region of 300 deg circumferential angle, and consequently to disadvantages in that region.

CONCLUSIONS

In the present paper, the flow pattern in an extraction module of an industrial steam turbine downstream the control valves is investigated numerically. The compact design of extraction modules causes a spatial non-uniformity in the mass flux distribution and incidence upstream of the guide vane row. Depending on the turbine size, the following suggestions should be taken into account, in order to improve inflow conditions:

- The valve seat should be positioned as far away as possible from the hub, in order to homogenise radial velocity distribution.
- Basically, control valves should be positioned tangentially to the hub, to ensure a direct inflow in the lateral sides of the inlet chamber as well as to distribute as much steam as possible in circumferential direction. A smaller centrally positioned additional valve and also a necking of the casing in flow direction could be useful too, to suppress a transition of the flow.

Since separation behaviour inside the diffusers is dependent of the valve hub, additional studies at different valve lifts should validate the results shown in this contribution. In order to investigate the transient blade loading of the reaction stages, simulation domain should be extended with the rotor blading. Subsequently in more detailed transient studies the spatial and time-dependent mechanical blade loading can be investigated. Hence, further work will focus on the flow pattern at different valve lifts as well as on the investigation of influence from the disturbed mass flux distribution upstream of the adjacent rotor blading, especially regarding mechanical blade loads.

ACKNOWLEDGEMENTS

The development work was conducted as a part of the joint research program COORETEC-turbo in the frame of AG Turbo. The work was supported by the Bundesministerium für Wirtschaft und Technologie (BMWi), as per resolution of the German Federal Parliament under grant number 0327717A. The authors gratefully acknowledge AG Turbo and MAN Diesel & Turbo SE for their support and permission to publish this paper. The responsibility for the content lies solely with its authors.

REFERENCES

- Greim, A., Havakechian, S., (1999), *Recent Advances in the Aerodynamic Design of Steam Turbine Components*, VGB-Fachtagung, 1999
- Hecker, S., (2011), *Strömungs- und strukturmechanische Untersuchung der Einströmung einer Dampfturbine*, doctoral thesis, Ruhr-Universität Bochum, Germany, 2011
- Kalkkuhl, T. J., Engelmann, D., Harbecke, U., Mailach, R., (2012), *Numerical Analysis of Partial Admission Flow in an Industrial Steam Turbine*, ASME Paper No. GT2012- 68465, ASME Turbo Expo, Copenhagen, Denmark, 2012
- Kocarnik, P., Jirku S. (2005), *The Design of Annular Bend in Spiral Casing of the Low-pressure Part Steam Turbines*, ETC Paper No. 047_10/122, Proceedings of 6th European Conference on Turbomachinery – Fluid Dynamics and Thermodynamics, Lille, France, 2005
- Kovats, A. (1979), *Effect of non-rotating passages on performance of centrifugal pumps and subsonic compressors*, Proceedings of the Winter-Annual Meeting, New York, USA, 1979

- Lüdtke, K. (1985), *Centrifugal process compressors – radial vs. tangential suction nozzles*, ASME Paper 85-GT-80
- Morita, R., Inada, F., Mori, M., Tezuka, K., Tsujimoto Y. (2004), *CFD Calculation and Experiments of Unsteady Flow on Control Valve*, ASME Paper No. HT-FED04-56017, ASME Heat Transfer/Fluids Engineering Summer Conference, Charlotte, North Carolina, USA, 2004
- Schlichting, H., (1979), *Boundary-layer theory*, Seventh Edition, McGraw-Hill Book Company, USA, 1979, pp. 729-757
- Sievert R., (2006), *Analyse der Einflussparameter auf die Strömung im Eintritt von Niederdruck-Dampfturbinen*, doctoral thesis, Ruhr-Universität Bochum, Germany, 2006
- Tajc, L., Bednar, L. Stastny, M., (2003); *Control Valves For Turbines of large Output*, Transactions of the Institute of Fluid-Flow Machinery, Vol. 114, pp. 209-218
- Traupel, W., (2001), *Thermische Turbomaschinen*, 4. Auflage, Springer, Berlin, Germany, 2001
- Van Den Braembussche, R.A., (2006), *Flow and Loss Mechanisms in Volute of Centrifugal Pumps*, Educational Notes RTO-EN-AVT-143 12 (2006), pp. 1-26
- Zhang D., Engeda, A., Hardin, J. R., Aungier, R. H., (2004), *Experimental study of steam turbine control valves*, Proceedings of the Institution of Mechanical Engineers, Vol. 218, Part C: Journal of Mechanical Engineering Science 2004, pp. 493-507